Chemically responsive molecular transistors fabricated by self-aligned lithography and chemical self-assembly

J. Tang,[a] Y. Wang, and C. Nuckolls
Center for Electron Transport in Molecular Nanostructures, Columbia University, New York, New York 10027 and Department of Chemistry, Columbia University, New York, New York 10027

S. J. Wind
Center for Electron Transport in Molecular Nanostructures, Columbia University, New York, New York 10027 and Department of Applied Physics and Applied Mathematics, Columbia University, New York, New York 10027

(Received 31 May 2006; accepted 21 August 2006; published 4 December 2006)

The authors present the fabrication and characterization of molecular transistors comprising at most a small number of molecules, which display a distinct chemical function. The fabrication involves a self-aligned technique capable of patterning metal electrodes with interelectrode separations of ~2 nm with very high yield. The electrodes are bridged by molecules with a metal-ion core which can be inserted by *in situ* designed chemical reaction. The presence or absence of the ion modulates the electrical conductance of the device. © *2006 American Vacuum Society.*
[DOI: 10.1116/1.2357968]

I. INTRODUCTION

The promise of molecular electronics[1] lies not only in the small size of the conducting channel, which suggests the possibility of integration levels far beyond those of present day technology, but also in the diversity of chemical structures that can be conceived and synthesized, offering a wide range of functionality. Thus, a molecular electronic device could, in principle, be used as an electronic switch that can also perform other tasks, such as molecular recognition or binding, with potential applications in sensing and chemical signal transduction. Highly conjugated organic molecules synthesized for such studies are no more than a few nanometers in length, and the reliable fabrication of electrodes that can be bridged by a single molecule remains a significant challenge.[2–4]

We have developed two new techniques for the fabrication and assembly of single-molecule transistors. The first technique involves the patterning of metallic electrodes separated by a nanoscale gap into which a single molecule may be inserted. This electrode fabrication technique is self-aligned, requiring no extraordinary lithographic capabilities. We have recently reported that this technique is capable of producing sub-10-nm gaps with very high yield.[5] Control of the interelectrode separation is determined by the oxidation of a thin sacrificial layer of Al, which is deposited directly upon the first electrode. In this work, we have extended this technique to produce devices with interelectrode gaps as small as ~2 nm.

The second technique involves *in situ* chemistry reaction inside the nanogap, which enables the chemical signal to be transduced as a change in electrical conductance of the molecule within the nanogap. By assembling a monolayer on metal electrode, the electrode surface is modified by the properties of the assembled molecule. This is done by functionalizing individual molecular units with appropriate end groups, such that they will selectively attach one end to the metal electrode while leaving the other end to be recognized by molecules or ions from solution or from another electrode. By assembling the molecules in this way, a given device may be designed with specific chemical or electrical functionality. In addition, the length of the molecule may be modified by this *in situ* assembly, relaxing the requirement that the molecule "fit" precisely in the interelectrode gap, thus making it easier to wire up conjugated molecules.

II. ELECTRODE FABRICATION

The critical steps for the self-aligned fabrication of the nanoelectrodes, shown schematically in Fig. 1, involve two separate lithographic patterning steps. Only gross (approximately micron scale) alignment is required between the two steps, as nanoscale precision is achieved by a self-aligned process.

Samples are fabricated on heavily doped (*n*-type) silicon substrates upon which a thin layer (~4–7 nm) of ZrO_2 has been deposited by atomic layer deposition. The substrate serves as a gate electrode,[6,7] and the ZrO_2 is the gate dielectric. Because of the high dielectric constant of ZrO_2 (~20–24), thicker films may be used relative to SiO_2 while achieving the same effective gate field coupling. ZrO_2 provides an additional advantage when Pt is used as the electrode material, in that Pt grows on ZrO_2 in two-dimensional sheets,[8,9] leading to extremely smooth Pt films which are conductive even at thicknesses of only a few nanometers.

The first step in the nanoelectrode formation process is the lithographic patterning of the first electrode. In the present work, this is done by electron beam lithography, although virtually any lithographic method may be used. A sample is coated with a layer of polymethylmethacrylate (PMMA) to a thickness ranging from ~25 to 120 nm, de-

[a]Electronic mail: jt2128@columbia.edu

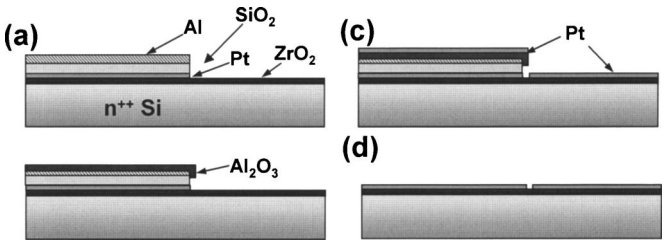

FIG. 1. Nanogap fabrication sequence. (a) First electrode patterning. A trilayer consisting of the first electrode metal (Pt), a layer of SiO_2, and a thin layer (~2–5 nm) of Al is deposited. (b) The Al is allowed to oxidize in air. (c) A second lithography and deposition step defines the second electrode (Pt). (d) The Al_2O_3, Al, and SiO_2 are stripped, leaving the two metal electrodes separated by a nanogap.

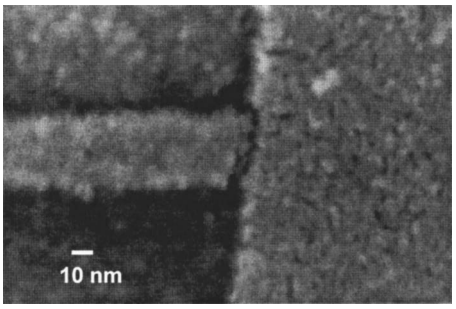

FIG. 2. SEM image of Pt electrodes separated by a gap of ~2–3 nm.

pending on the thickness of the metal to be deposited. Exposure of the first electrode pattern is done in an FEI Sirion scanning electron microscope (SEM) equipped with a pattern generator and control system from J. C. Nabity, Inc. The first electrode pattern typically consists of an array of rectangles with dimensions of ~1 μm or less on a side. This enables easy alignment of the second electrode pattern in a subsequent lithographic exposure.

Following exposure and PMMA development, the first electrode pattern is deposited as a trilayer consisting of the electrode metal (Pt), followed by sacrificial layers of SiO_x and Al. All three layers are deposited *in situ* by electron beam evaporation without breaking vacuum. The SiO_x and Al film thicknesses are typically ~5 and 2–5 nm, respectively, as determined by a quartz crystal microbalance. After removal from the electron beam evaporator, the sample undergoes lift-off in a mixture of CH_2Cl_2 and acetone (9:1) at 75 °C with mild ultrasonic agitation. The first electrode pattern covered by the sacrificial layer is shown schematically in Fig. 1(a). Al oxidizes easily in air and is known to form a robust native oxide layer with thickness of a few nanometers[10] [Fig. 1(b)], resulting in an overhang structure on top of the first electrode, while the SiO_x and Al form an ideal bilayer profile for a subsequent lift-off process. (It may be possible to oxidize the Al film *in situ* prior to removal of the sample from the electron beam evaporator. This may afford improved control over the thickness of the aluminum oxide.) Because of the thinness of the Al oxide layer, it has been somewhat difficult to determine the precise thickness of the oxide layer by standard ellipsometric and scanning electron microscope techniques,[10] although efforts continue to further characterize these films via high resolution transmission electron microscopy (HRTEM).

The second electrode is patterned by electron beam lithography using a process similar to the first electrode patterning. The pattern is coarsely aligned to the first electrode using prepatterned alignment marks. The second electrode pattern consists of rectangles similar to those in the first electrode pattern, although they may be narrower in one dimension, in order to limit the number of molecules that will assemble between the electrodes. (In this work, the second electrode width is chosen to be ~20 nm.) The narrow second electrode pattern runs across the first electrode, as in Fig. 1(c). The electron channel of the transistor will be formed at the intersection of the two rectangles.

Following exposure and development of the second electrode pattern, a second metal film is deposited by electron beam evaporation. The metal may be the same as the first electrode material or it may be different. For this work, we have chosen to form the second electrode from Pt. The *thickness* of the second electrode is critical. It cannot be substantially thicker than the first electrode, as it will tend to form on the sidewall of the Al film, making it difficult to remove when the Al and SiO_x are stripped. After the second electrode metal deposition, the sample undergoes another lift-off step similar to that used for the first electrode patterning. This leaves a narrow strip of metal running across the first electrode.

At this point in the process, the Al and SiO_x sacrificial layers are removed by immersion in an etchant solution. In the case of Pt on ZrO_2, the sacrificial layers are removed in an aqueous solution of tetramethylammoniumhydroxide, followed by a H_2O rinse. This step removes the Al, Al_2O_3,

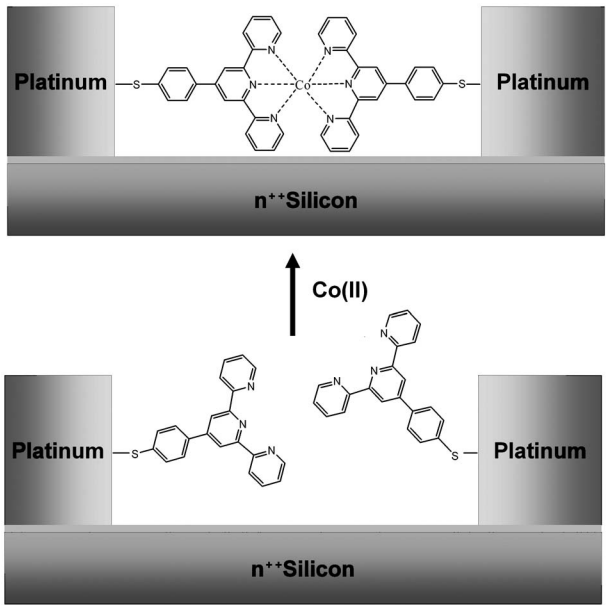

FIG. 3. Schematic diagram of chemical functionalization of the terpyridyl molecule attached to Pt electrodes. Top: After treatment in $Co(OAc)_2$. The complex end to end is ~3 nm long.

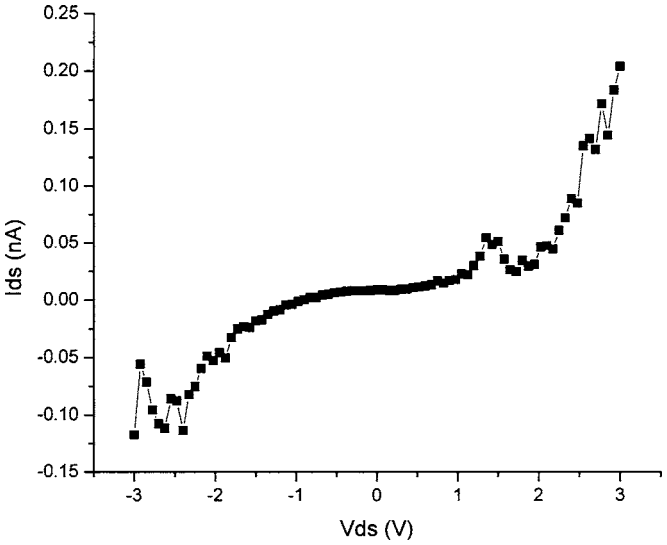

FIG. 4. As-made nanogap devices show tunneling current.

SiO_x, and the second layer of metal which was patterned on top of the first electrode, as shown in Fig. 1(d). The yield of this process in terms of the number of devices on a sample with nanometer-spaced electrodes as a function of devices patterned is extremely high, ~80%. A scanning electron micrograph of a device with interelectrode spacing of ~3 nm is shown in Fig. 2.

As mentioned previously, cross-sectional TEM analysis is required to establish a definite correlation between the gap width and the Al thickness. At this point, however, we can rule out the possibility that the gap is formed by shadow effects due to angled evaporation across the edge of the Al film, which would require a 16° angle to achieve 3 nm gap with a 10-nm-thick film (the source to substrate distance is ~1 m in our evaporator). Furthermore, the reproducibility of the gaps that we have achieved apparently rules out random variations of such a shadow angle during evaporation.

III. MOLECULAR ASSEMBLY AND ELECTRICAL MEASUREMENT

The molecule used in this work is thiolated terpyridine derivative shown in Fig. 3. When mixed with Co^{2+} solution, two [tpy-SH] molecules will combine with one Co^{2+} to form a dimer $[Co(tpy\text{-}SH)_2]^{2+}$. In this work, this chemical reaction is performed inside the prefabricated nanogaps, while the tpy-SH molecules are immobilized on platinum electrodes. The electrical response of the device monitors the chemical reaction of single or few molecules inside the nanogap.

The prefabricated platinum nanogaps are electrically tested prior to and after the tpy-SH assembly in order to ensure that no conductive channel is formed upon the initial tpy-SH. Initial room temperature measurements on bare electrodes (i.e., without the presence of any molecule) detect a tunneling current in ~15% of the devices, as shown in Fig. 4. This is a good indication that the interelectrode spacing for these devices is ~2 nm or less.[11,12] The devices are then tested after the assembly of the tpy-SH. Currents of the devices on this step are recorded to compare with following steps. Most devices show no substantial current increase, as indicated in Fig. 5(a), while a small fraction shows some unstable increasing current; this may due to the tunneling between molecules. When the devices are then placed into a solution of $Co(OAc)_2$ in H_2O, removed, rinsed, and again measured, 25 out of 110 devices show an increase in current of approximately three orders of magnitude [Fig. 5(b)]. This indicates the connection of two terpyridyl arms via a Co^{2+} connection. Details of the chemical assembly and electrical results will be provided in a separate publication.[13]

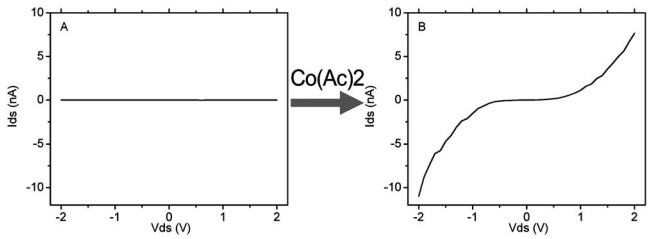

FIG. 5. Output characteristics of terpyridyl device after sequential chemical treatments. (a) After assembly of terpyridyl on Pt electrodes. (b) After 72 h in $Co(OAc)_2$ solution.

IV. CONCLUSIONS

We have demonstrated a new method for fabricating electrodes for probing single molecules. The method is completely self-aligned, relying upon the oxidation of a thin layer of Al to determine the size of the interelectrode gap. Using *in situ* assembly of molecules between these electrodes, we observe electron transport through these molecules and successfully realized chemical response on these molecular devices which may be generalized to other chemical as well as biological systems.

[1] A. Aviram and M. A. Ratner, Chem. Phys. Lett. **29**, 277 (1974).
[2] M. D. Fischbein and Marija Drndić, Appl. Phys. Lett. **88**, 063116 (2006).
[3] E. P. De Poortere, H. L. Stormer, L. M. Huang, S. J. Wind, S. O'Brien, M. Huang, and J. Hone, Appl. Phys. Lett. **88**, 143124 (2006).
[4] L. Qin, S. Park, L. Huang, and C. A. Mirkin, Science **309**, 113 (2005).
[5] J. Tang, E. P. De Poortere, J. E. Klare, C. Nuckolls, and S. J. Wind, Microelectron. Eng. **83**, 1706 (2006).
[6] S. J. Tans, A. R. M. Verschueren, and C. Dekker, Nature (London) **393**, 49 (1998).
[7] R. Martel, T. Schmidt, H. R. Shea, T. Hertel, and P. Avouris, Appl. Phys. Lett. **73**, 2447 (1998).
[8] S. Roberts and R. J. Gorte, J. Phys. Chem. **95**, 5600 (1991).
[9] P. A. Dilara and J. M. Vohs, J. Phys. Chem. **99**, 17259 (1995).
[10] A. Bachtold, P. Hadley, T. Nakanishi, and C. Dekker, Science **294**, 1317 (2001).
[11] E. P. De Poortere, H. L. Stormer, L. M. Huang, S. J. Wind, S. O'Brien, M. Huang, and J. Hone, Appl. Phys. Lett. **88**, 143124 (2006).
[12] J. G. Simmons, J. Appl. Phys. **346**, 1793 (1963).
[13] J. Tang, Y. Wang, J. E. Klare, S. J. Wind, and C. Nuckolls (unpublished).